Preprints of the 18th IFAC World Congress
Milano (Italy) August 28 - September 2, 2011

Two-Stage Optimal Control of a Parallel Hybrid Vehicle with Traffic Preview

Tae Soo Kim*, Chris Manzie and Rahul Sharma

*Department of Mechanical Engineering, The University of Melbourne, VIC 3010, Australia (*e-mail: t.kim2@pgrad.unimelb.edu.au)*

Abstract: An approach for the optimal control of both velocity and torque split of a parallel hybrid electric vehicle with traffic preview is presented in this paper. The optimal controller is analytically derived using Pontryagin's Minimum Principle. The optimal velocity and torque split trajectories developed are then repeatedly recalculated in a receding horizon fashion over drive cycles to assess the potential fuel saving with varying lengths of the traffic preview.

Keywords: two-stage optimal control, hybrid vehicle, vehicle telemetry

1. INTRODUCTION

In a climate of increasing concern about fuel economy and greenhouse gas emissions, hybrid electric vehicles (HEV) are increasingly popular with consumers and manufacturers alike. The superior fuel economy of an HEV is achieved with added functionality provided by an electric motor, including engine shutoff at idle and regenerative braking, but without sacrificing range as in the case of pure electric vehicles.

The control strategy that determines the combination between engine and motor at different stages of a trip is well known to significantly impact the overall fuel consumption, while controlling velocity in a trip without compromising the arrival time, may fully exploit potential fuel savings of an HEV. The optimal control of these two aspects requires future traffic information *a priori*, which may be obtained using a network of vehicular telemetry devices as discussed in (Zhuang et al., 2008).

Pisu and Rizzoni (2007) applied HEV torque split control with telemetry information, based on the equivalent consumption minimisation strategy (ECMS) proposed in Sciarretta et al. (2004). Other approaches included model predictive control (MPC), in which dynamic programming technique is used to solve the finite horizon problem as in (Back et al., 2004) and (Johannesson and Egardt, 2007). The latter work showed up to 2% fuel improvement over a flat road, but by only addressing torque split, the approaches did not fully maximise the potential fuel saving for an HEV.

More recently, Manzie et al. (2007) demonstrated fuel saving by managing a vehicle's velocity using an essentially ad-hoc approach given limited traffic information ahead and Hellstrom et al. (2010) studied fuel saving with velocity control for a heavy truck by utilising road topography. It was indicated that there is further potential fuel economy improvement in an HEV velocity control in conjunction with torque split control.

Building on this prior work, Kim et al. (2009) integrated the torque split and velocity control of an HEV over a flat road profile using nonlinear MPC. The work showed 6.6% fuel economy improvement relative to a benchmark rule-based controller with traffic preview as short as 5 seconds. However the computational burden for solving the nonlinear optimisation was a major drawback, and highlighted a need for computationally efficient algorithms. A similar problem was tackled by van Keulen et al. (2010) for a hybrid electric truck in the highway driving scenario with varying road topography. However, the authors treated velocity control and the torque split control as decoupled problems, and the optimality as a combined problem was not discussed.

As a computationally effective alternative to Kim et al. (2009), Pontryagin's minimum principle (PMP) is considered in this work, to find the analytical solution for the fuel optimal torque split and velocity control of an HEV in the presence of limited traffic preview and using simplifying assumptions. To solve this problem, two-stage optimal control (Tomiyama, 1985) is used. The formulation is then applied on a high fidelity vehicle model over a drive cycle with limited preview horizon, ensuring the same arrival time as the traffic, but avoiding unnecessary depletion of battery's charge level.

2. A CONTROL ORIENTED HEV MODEL

An HEV is a complex dynamic system with highly nonlinear subcomponents. A simpler mathematical model which attempts to capture the key HEV characteristic is adopted for the controller development in this work and is presented in this section.

2.1 Vehicle and Engine Dynamics

Single dimensional forward motion is considered for modelling the vehicle dynamics. The external dynamics of the vehicle velocity, $v(t)$ and position $d(t)$ are thus given as

$$\frac{d}{dt}v(t) = \frac{1}{m}[F(t) - c_0 - c_2 v(t)^2] \tag{1}$$

$$\frac{d}{dt}d(t) = v(t) \tag{2}$$

where c_0 and c_2 are positive constants representing drag coefficients.

The total applied force $F(t)$ is constrained to the range, $F \in [-F_{b,max}, F_{d,max}]$, where $F_{b,max}$ and $F_{d,max}$ are positive numbers representing maximum braking and driving forces, respectively. Depending on the nature of applied force, the vehicle state is classified into three possible phases, namely, acceleration phase, deceleration phase or coasting phase. When $F > 0$, the vehicle is denoted to be in an *acceleration phase*, where the total driving force comes from the combination of the engine and electric motor. When $F < 0$, the vehicle is denoted to be in a *deceleration phase*, braking with a combination of friction and regenerative braking. When $F = 0$ the vehicle is said to be in a *coasting phase*, where the velocity changes only due to frictional and aerodynamic effects.

During the acceleration phase, the engine and motor combine to produce the driving force, which is proportionally related to the total driving torque.

$$F(t) = c_3 \tau_{total}(t) \tag{3}$$

where c_3 is a constant reflecting fixed gear ratio.

The torque split ratio u is defined as the ratio of the torque produced by the engine, τ_{eng} to the total torque required for the vehicle, τ_{total}, and following from (3), it is the ratio of the force produced by the engine, F_{eng} to the total force required:

$$u(t) = \frac{\tau_{eng}(t)}{\tau_{total}(t)} = \frac{F_{eng}(t)}{F(t)} \tag{4}$$

where the range of u is $u \in [0, u_{max}]$. The parallel HEV mode of operation during the acceleration phase is defined based on the value of u:

- $u = 0$: pure electric mode
- $0 < u < 1$: hybrid mode
- $u = 1$: pure engine mode
- $1 < u < u_{max}$: recharging mode

During deceleration, the clutch disengages the engine from the drive line. The electric motor alone remains engaged to recuperate energy and thus acts as a load torque. Hence u is undefined during the deceleration phase.

The following assumption is now made regarding the engine used in the HEV model described in (1) - (4):

Assumption 1. The fuel consumption of the vehicle is linearly proportional to the engine power output.

A similar assumption has also been used by Guzzella and Sciarretta (2007) for modelling conventional vehicles, and ignores any nonlinearity in engine efficiency maps. By extending the assumption to hybrid vehicles in this work, the implication is that during pure electric mode, coasting or braking operation the engine is assumed to be turned off rather than idling. Furthermore, as no gearing exists in the model (3), it is clear that the fuel consumption will rise monotonically with vehicle velocity.

2.2 Electrical System

In modelling the electrical system of the vehicle, the following assumption is made:

Assumption 2. The electricity consumption of the vehicle is linearly proportional to the electric motor power output.

This is equivalent to Assumption 1, in that any nonlinearities in the motor efficiency maps are ignored during the acceleration phase. Furthermore, it implies that there is no dependency on the rate of change of battery state of charge due to the state of charge level. While this latter point is not true across the entire operating range of the battery, it will be reasonable if the fluctuations in state of charge are small, as is typically the case.

Under Assumption 2, the dynamics of the battery state of charge during the acceleration phase may be represented by:

$$\frac{d}{dt}q(t) = -c_4(1 - u(t))F(t)v(t) \quad , \qquad F \geq 0 \tag{5}$$

where c_4 is a positive constant that reflects motor/generator efficiency. It is worth noting that (5) applies for $0 < u \leq u_{max}$. During the deceleration phase, only the fraction of braking power captured regeneratively, R, can accumulate the state of charge since the engine disengages from the driveline. In this work R is assumed constant throughout all braking events, leading to the state of charge dynamics during deceleration being represented by:

$$\frac{d}{dt}q(t) = -c_4 R F(t)v(t) \quad , \qquad F \leq 0 \tag{6}$$

3. PROPOSED OPTIMAL CONTROLLER

Given that the problem of determining optimal velocity and torque split is a multivariable optimization problem and there are constraints associated with the HEV states, Pontryagin's Minimum Principle (PMP) represents a good candidate methodology to establish an analytical solution. However, the two phases of the battery state of charge dynamics caused by acceleration and deceleration, as per (5) and (6), imply that standard form of Pontryagin's technique is not applicable in the case at hand, and an alternative approach is sought. To this end, a two stage Pontryagin's Minimum Principle approach of Tomiyama (1985) is applied on HEV model (1)-(6) so as to develop a multivariable optimal controller which minimizes the fuel consumption over a finite length of traffic preview.
The following assumption is used in ensuing analysis.

Assumption 3. The telemetry provides a limited preview of the traffic ahead *a priori* and furthermore is sufficiently short that the optimal trajectory may be represented using only two phases separated by a coasting phase.

Limiting the number of phases in the segment to two allows a two-stage optimal control approach formulated in Tomiyama (1985) to be applied.

3.1 Review of Two-stage Optimal Control, Tomiyama (1985)

Consider the state vector, $\mathbf{x}$, whose dynamics over the period $[t_0, t_f]$ change from f_1 to f_2 at time t_1, i.e.

$$\frac{d\mathbf{x}}{dt} = \begin{cases} f_1(\mathbf{x}, \mathbf{u}, t) & [t_0, t_1) \\ f_2(\mathbf{x}, \mathbf{u}, t) & (t_1, t_f] \end{cases} \tag{7}$$

The cost J for the combined two stages is defined to be:

$$J(\mathbf{x}, \mathbf{u}, t, t_1) = \int_{t_0}^{t_1} L_1(\mathbf{x}, \mathbf{u}, t)\, dt + \int_{t_1}^{t_f} L_2(\mathbf{x}, \mathbf{u}, t)\, dt \tag{8}$$

where L_1 and L_2 are the integrands of costs of the first phase and the following phase respectively. The variables that can be chosen to minimise the cost are the control vector, $\mathbf{u}$, and the switching time, t_1.

The corresponding Hamiltonians H_i for each phase are given as

$$H_i(\mathbf{x},\mathbf{p},\mathbf{u},t) = L_i(\mathbf{x},\mathbf{u},t)+\mathbf{p}^T f_i(\mathbf{x},\mathbf{u},t), \qquad i=1,2 \quad (9)$$

where $\mathbf{p}$ is vector of costate variables.

If * is used to designate optimality of a variable, the two necessary conditions for optimality of a two-stage optimal problem may be stated as follows:

(1) The optimal control at each stage minimises the Hamiltonian for the corresponding stage.

$$\min_{\mathbf{u}_1} H_1(\mathbf{x}^*(t),\mathbf{p}_1^*(t),\mathbf{u}_1(t),t) \quad (10)$$
$$= H_1(\mathbf{x}^*(t),\mathbf{p}_1^*(t),\mathbf{u}_1^*(t),t), \quad t_0 \le t < t_1$$

$$\min_{\mathbf{u}_2} H_2(\mathbf{x}^*(t),\mathbf{p}_2^*(t),\mathbf{u}_2(t),t) \quad (11)$$
$$= H_2(\mathbf{x}^*(t),\mathbf{p}_2^*(t),\mathbf{u}_2^*(t),t), \quad t_1 < t \le t_f$$

(2) The costate variables and the Hamiltonian should be continuous at the switching time t_1, i.e.

$$\mathbf{p}^*(t_1^{*-}) = \mathbf{p}^*(t_1^{*+}) \quad (12)$$

$$H_1(\mathbf{x}^*(t_1^*),\mathbf{p}^*(t_1^*),\mathbf{u}_1^*(t_1^*),t_1^*) \quad (13)$$
$$= H_2(\mathbf{x}^*(t_1^*),\mathbf{p}^*(t_1^*),\mathbf{u}_2^*(t_1^*),t_1^*)$$

3.2 Analysis of Acceleration Phase: $F \ge 0$

In order to develop a cost function minimising energy, it is necessary to introduce a fuel-electricity equivalence ratio, K, which depends on efficiencies of engine and motor. The equivalence factor weights the use of electric power against fuel power. When K is less than one, it follows that electric energy is favourable relative to fuel and, when K is greater than one, use of electric energy is penalised.

Assumption 4. The equivalence factor K is constant over the interval $t \in [t_0, t_f]$.

In reality, the electric to fuel energy equivalency varies with engine and motor operating point. However a constant equivalence factor is reasonable for small perturbations from the current operating point, which is consistent with relatively short trip segments. The value of K may be refreshed with every new interval.

As a consequence, the cost function during the acceleration phase, J_a, in a finite time interval $[t_a, t_b]$ may be written as the following equation:

$$J_a(\mathbf{x},\mathbf{u},t) = \int_{t_a}^{t_b} u(t)F(t)v(t) + K(1-u(t))F(t)v(t)\,dt \quad (14)$$

The Hamiltonian for the acceleration phase is formed by substituting (1), (2), (5) and (14) into (9).

$$H_a(\mathbf{x},\mathbf{u},\mathbf{p},t) = u(t)F(t)v(t) + K(1-u(t))F(t)v(t) + \frac{p_1(t)}{m}[F(t) - c_0 - c_2 v(t)^2] + p_2(t)v(t) - p_3(t)c_4(1-u(t))F(t)v(t) \quad (15)$$

where $p_1(t)$, $p_2(t)$ and $p_3(t)$ are the costate variables.

From (10) a necessary condition for $\mathbf{u}^*$ to be optimal is

$$H_a(\mathbf{x}^*,\mathbf{u}^*,\mathbf{p}^*,t) \le H_a(\mathbf{x}^*,\mathbf{u},\mathbf{p}^*,t) \quad (16)$$

and the corresponding dynamics of the costates are:

$$\dot{p_1}^*(t) = -\frac{\partial H_a}{\partial v} = -u^*(t)F^*(t) - K(t)(1-u^*(t))F^*(t) + \frac{2p_1^*(t)c_2v^*(t)}{m} - p_2^*(t) + p_3^*(t)c_4(1-u^*(t))F^*(t) \quad (17)$$

and the optimal costates p_2^* and p_3^* are constants.

Substituting the Hamiltonian (15) into the inequality (16) results in the inequality:

$$u^*(t)F^*(t)[v^*(t) - \sigma(t)v^*(t)] + F^*(t)[\sigma(t)v^*(t) + \frac{p_1^*(t)}{m}] \le u(t)F(t)[v^*(t) - \sigma(t)v^*(t)] + F(t)[\sigma(t)v^*(t) + \frac{p_1^*(t)}{m}] \quad (18)$$

where $\sigma(t) := K - c_4 p_3^*(t)$. Further define the following transformed co-state variables β_1 and β_2 as

$$\beta_1(t) := v^*(t) - \sigma(t)v^*(t) \quad (19)$$

$$\beta_2(t) := \sigma(t)v^*(t) + \frac{p_1^*(t)}{m} \quad (20)$$

Now (18) can be written in terms of u and F_d as:

$$F^*(t)[u^*(t)\beta_1(t) + \beta_2(t)] \le F(t)[u(t)\beta_1(t) + \beta_2(t)] \quad (21)$$

$F(t)$ is non-negative since the minimum driving force applied on the vehicle during acceleration is zero. $u(t)$ is also non-negative since the engine cannot produce a negative torque, hence $u_{min} = 0$. With these non-negative u and F, decision planes on the switching instances with respect to β_1 and β_2 can be deduced.

$$F^*(t) = 0, \qquad u(t)\beta_1(t) + \beta_2(t) > 0 \quad (22)$$
$$F^*(t) = F_{d,max}, \qquad u(t)\beta_1(t) + \beta_2(t) < 0 \quad (23)$$

This decision plane is represented graphically in the costate space by the dotted line in Figure 1 and trajectories defined by the solutions of (17)-(20).

Since both $F(t)$ and u are non-negative, solving the inequality (21) leads to the following decision plane which is represented by the dashed line in Figure 1:

$$u^*(t) = u_{min}, \qquad \beta_1(t) > 0 \quad (24)$$
$$u^*(t) = u_{max}, \qquad \beta_1(t) < 0 \quad (25)$$

There is also a singular case when $\beta_1(t) = 0$ and $\beta_2(t) = 0$ for $t \in [t_a, t_b]$ and no information can be obtained from the Hamiltonian inequality. Since β_2 is zero and remains zero in this interval,

$$\beta_2(t) = \sigma(t)v^*(t) + \frac{p_1^*(t)}{m} = 0$$
$$\dot{\beta}_2(t) = \dot{\sigma}(t)v^*(t) + \sigma(t)\dot{v}^*(t) + \frac{\dot{p}_1^*(t)}{m} = 0 \quad (26)$$

The conditions $\beta_1(t) = 0$ and $\dot{\beta}_1(t) = 0$ give $\sigma(t) = 1$ and $\dot{\sigma}(t) = 0$. The problem reduces down to a conventional vehicle problem when travelling in a singular arc, and the optimal speed of the vehicle is found to be constant during this period. A detailed analysis using a non-hybrid vehicle model is found in Stoicescu (1995) and Appendix I of Guzzella and Sciarretta (2007).

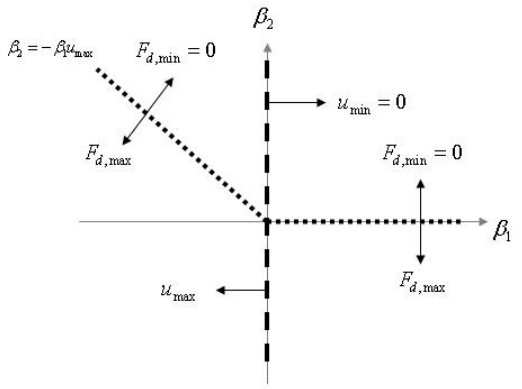

Fig. 1. Decision planes for optimal inputs during acceleration phase on β_1-β_2 plane

3.3 Analysis of Deceleration Phase: $F \leq 0$

During deceleration, the engine disengages and switches off, hence there is no power blending between engine and motor. Therefore the problem is reduced to a single control variable, the braking force, F. The fuel consumption problem during this phase can therefore be formulated as maximising the energy captured through regenerative braking, which is expressed by the following cost function to be minimised:

$$J_d(\mathbf{x}, \mathbf{u}, t) = \int_{t_a}^{t_b} -KRF(t)v(t)\,dt \tag{27}$$

subject to the distance requirement and specified final velocity.

From (27), the Hamiltonian for the decelerating phase is:

$$\begin{aligned} H_d(\mathbf{x}, \mathbf{u}, \mathbf{p}, t) = &- KRF(t)v(t) + \frac{p_1(t)}{m}[F(t) - c_0 - c_2 v(t)^2] \\ &+ p_2(t)v(t) - p_3(t)c_4 RF(t)v(t) \end{aligned} \tag{28}$$

The dynamics of the costate variables are:

$$\begin{aligned} \dot{p_1}^*(t) = &-KRF^*(t) + \frac{2p_1^*(t)c_2 * v^*(t)}{m} \\ &- p_2^*(t) + p_3^*(t)c_4 RF^*(t) \end{aligned} \tag{29}$$

and p_2^* and p_3^* are constants.

Substituting (28) into (16) results in

$$F^*(t)\beta_3(t) \leq F(t)\beta_3(t) \tag{30}$$

where

$$\beta_3(t) := -KRv^*(t) + \frac{p_1^*(t)}{m} + p_3^*(t)c_4 Rv^*(t) \tag{31}$$

From (30) the following result can be deduced,

$$\begin{aligned} F^*(t) &= -F_{b,max},\ \beta_3(t) > 0 \\ F^*(t) &= 0,\ \beta_3(t) < 0 \end{aligned} \tag{32}$$

The optimal inputs for the independent acceleration and deceleration phases have been found by treating them as two separate problems and applying Pontryagin's Minimum Principle. In all cases, the optimal control inputs are found to be *'bang-bang'*, switching between two extremes. The switching instance depends on β_1, β_2 and β_3, which include the unknown costate variables. The result resembles the bang-bang control structure found for the optimal torque split analysis in Wei et al. (2007).

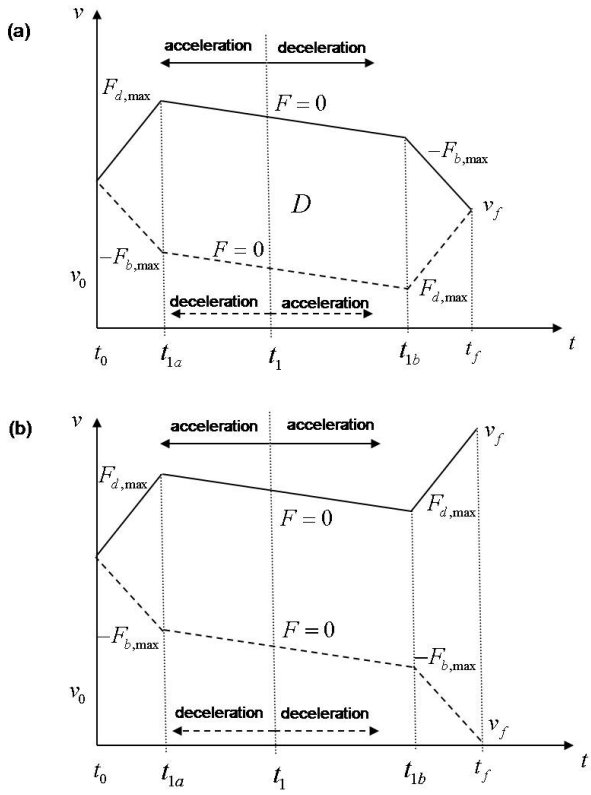

Fig. 2. Possible optimal velocity trajectories. (a) Acceleration followed by deceleration (solid), deceleration followed by acceleration (dashed). (b) Acceleration followed by acceleration (solid), deceleration followed by deceleration (dashed).

The optimal switching time for u^* and F^* can be calculated numerically solving for the costates while satisfying boundary conditions on $\mathbf{x}(0)$ and $\mathbf{x}(t_f)$. However this approach is a computationally difficult problem.

As a computationally favourable alternative, the shapes of the optimal input trajectories obtained from the acceleration and deceleration phase analysis are used together with Assumption 3 to develop two-stage optimal control trajectories over the time horizon corresponding to the traffic preview length. In conjunction with the boundary conditions on the states, the next section pursues this option of determining the optimal trajectory.

3.4 Combined phases with boundary conditions

The optimal control inputs of the individual acceleration and deceleration phases satisfy conditions (10) and (11), respectively. Then, the optimal solution to the two-stage problem is obtained by combining the individual optimal solutions of Stages 1 and 2 of the two-stage PMP, where both Stages 1 and 2 can take either acceleration phase or deceleration phase as per (8). Four two-stage combinations are possible, as shown in Figure 2. The combination to obtain the final optimal control trajectories is governed by the determination of an optimal switching instant t_1 such that optimality conditions (12) and (13) hold.

The determination of t_1 in the case at hand is performed by applying optimal control inputs, obtained in Sections 3.2

and 3.3, on the HEV model (1)-(6) in conjunction with the boundary conditions with respect to on velocity, v_0 and v_f, total distance travelled, D, and terminal state of charge, q_f, over a known horizon interval $[t_0, t_f]$. For a given set of boundary conditions, only one out of the four trajectories in Figure 2 results in a feasible solution, satisfying all the boundary conditions. It may be noted that as per (1), the dynamics of v are completely independent of control u and state q and therefore the velocity trajectory can be worked out solely using F^* and the boundary conditions.

The resulting velocity trajectory links the two stages via a coasting phase, which is characterised by $F^* = 0$ from acceleration and deceleration phases. Clearly, the optimal switching instant lies in between t_{1a}, t_{1b} which are the starting and end time of the cruising phase, respectively. As a result the problem of determining optimal t_1 reduces to that of determining the optimal t_{1a} and t_{1b} such that the boundary conditions are satisfied. Furthermore, it is easy to verify the conditions (12) and (13) hold along the cruising phase implying the two stage optimality of the resulting solution.

From (24) and (25), it is known that u^* switches between u_{max} and u_{min}. Having now determined the velocity profile, it can be used to determine u^* based on the boundary conditions of the battery state of charge. During the coasting phase i.e. $t \in [t_{1a}, t_{1b}]$, electric energy is neither being used nor charged, hence the battery state of charge is constant. The amount of kinetic energy absorbed through regenerative braking is dependent on the duration of the deceleration phase. Accounting for the state of charge increase during the deceleration phase, the switching time for torque split during the acceleration phase can be adjusted to meet q_f.

3.5 Application in Receding Horizon

As an HEV equipped with telemetry moves forward with traffic, telemetry provides a new set of traffic information at each sampling period. Since telemetry can only supply limited feed-forward traffic information as stated in Assumption 3, and as time increments, so too does the available information, it is natural to update periodically (based on the update rate of the telemetry) the optimal control sequences and hence the optimal control trajectories based on the new traffic information.

Accordingly, the control approach proposed in Section 3.4 is used at each sampling instant to solve a finite horizon optimal control problem, subject to the constraints associated with the states (v, d, q) and control inputs (u, F). The optimal control trajectories (u^*, F^*) computed for a given set of telemetry information are only applied for the duration of sampling period. When the next set of the traffic preview information becomes available, the optimal control trajectories based on new information are recalculated, and this process is repeated resulting in a receding horizon control (RHC).

The application of *'bang-bang'* control scheme in practice is not desirable in the drivability point of view. To overcome this problem, the controller can be refreshed at a faster sampling frequency with a low pass filtering of the control input to obtain a smoother acceleration/deceleration.

Table 1. High order model parameters

Total weight	1800 kg
Frontal area	2.04 m^2
Coefficient of drag	0.33
Engine max. power	110kW
Motor max. power	59kW
Battery open circuit voltage	300V
Battery capacity	25 Ah
Transmission	Manual, 5spd
Gear ratios	3.57:2.00:1.33:1:0.75
Engine	Downsized GM 3800 Series II L36 engine
Motor	59kW AC induction motor

4. SIMULATION RESULTS

Simulations are conducted using ADVISOR with telemetry preview lengths of up to 30 seconds. A detailed model of HEV based on a medium-large sized family sedan is simulated in ADVISOR (Wipke et al., 1999), of which key vehicle specifications are as in Table 1. In order to simulate realistic driving conditions, two drive cycles, the US-FTP and the Australian Urban Drive Cycle (AUDC) are considered. The vehicle without telemetry has fuel economy of 7.5 and 7.9 $L/100km$ on each cycle respectively. Each drive cycle is examined for two different traffic cases: in the first case the simulated vehicle may overtake surrounding traffic, which may be considered representative of multiple vehicles coordinating their velocities. In the second case overtaking is prevented so as to simulate only the single vehicle with any preview information, and is modelled by imposing the constraint $F_{d,max} = F_{d,traffic}$ when vehicle separation is at its minimum allowable limit.

An example of the control trajectories in traffic following the US-FTP cycle with a preview length of 15 second and overtaking prevented is shown in Figure 3.

Despite being based on the reduced order model of Assumptions 1 and 2, the proposed controller with telemetry improves fuel economy for the detailed model over a drive cycle by adjusting its velocity as shown in Figure 3(a). The velocity is controlled with only three choices of forces which are $F_{d,max}$, $F = 0$, and $-F_{b,max}$. Smoothing of velocity is evident, and the vehicle exhibits an earlier deceleration and long coasting to avoid a complete stop and accelerates together with the traffic following coasting.

Although Assumption 2 does not hold in this simulation, the battery state of charge at the end of the trip returns to near the initial value of 0.7, as shown in Figure 3(b). This is achieved with the torque split command switching between u_{min} and u_{max}. The frequency of switching between u_{min} and u_{max}, i.e. engine on-off behaviour, can be constrained in real application as mentioned in Sciarretta et al. (2004) but has not been undertaken here. The battery state of charge is maintained near the desired level by constraining q_f at the end of each horizon. One possible drawback is that this method does not use much of the available energy stored in battery at this short preview. Alternatively, this may indicate the battery size could be decreased.

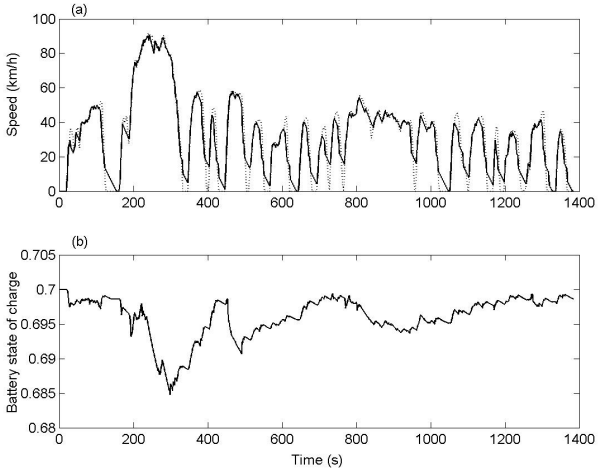

Fig. 3. Results from simulation of proposed control in traffic following the US-FTP cycle with 15 second traffic preview, position is constrained. (a) Optimal velocity profile (solid) and US-FTP cycle (dotted). (b) Battery state of charge fluctuation.

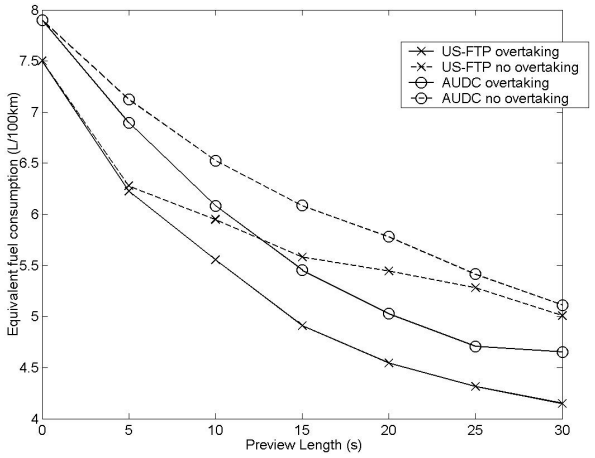

Fig. 4. Comparison of equivalent fuel consumption over US-FTP and AUDC, over a range of traffic preview length. Overtaking allowed (solid), overtaking disallowed (dashed).

The simulations were repeated for telemetry preview lengths ranges from 0 to 30 seconds for the two overtaking scenarios and the results are shown in Figure 4. Note that due to Assumption 2 no longer being valid, the final battery charge is often different to its initial condition and consequently is converted to a fuel-equivalent energy in $L/100km$. The average engine and motor efficiency throughout the drive cycle are used in the correction.

Figure 4 shows that there is clear fuel economy improvement as longer previews are applied. In both US-FTP and AUDC cycles, greater fuel saving is observed when the constraint on overtaking is not imposed. The margin of improvement is greater at short previews, and the improvement is less as the preview gets longer. The general decreasing trend is the same for other drive cycles, however the percentage of improvement depends on the frequency of start-stop behaviour present in the original cycle and the level of velocity smoothing acquired.

Simulations performed in ADVISOR have shown the improvement in fuel economy using the proposed controller over a range of preview lengths considered. Even though the controller is based upon the simple control oriented model presented in Section 2, uniform improvement in fuel economy is observed throughout the range of preview lengths. The proposed controller is shown to be insensitive to the modelling inaccuracy, and is a computationally effective alternative numerical optimisation based approaches.

REFERENCES

Back, M., Terwen, S., and Krebs, V. (2004). Predictive powertrain control for hybrid electric vehicles. In *IFAC Symposium on Advances in Automotive Control*.

Guzzella, L. and Sciarretta, A. (2007). *Vehicle Propulsion Systems. Introduction to Modeling and Optimization*. Springer, 2nd edition.

Hellstrom, E., Aslund, J., and Nielsen, L. (2010). Design of an efficient algorithm for fuel-optimal look-ahead control. *Control Engineering Practice*.

Johannesson, L. and Egardt, B. (2007). A novel algorithm for predictive control of parallel hybrid powertrains based on dynamic programming. In *Fifth IFAC Symposium on Advances in Automotive Control*.

Kim, T., Manzie, C., and Sharma, R. (2009). Model predictive control of velocity and torque split in a parallel hybrid vehicle. In *IEEE International Conference on Systems, Man, and Cybernetics*.

Manzie, C., Watson, H., and Halgamuge, S. (2007). Fuel economy improvements for urban driving: Hybrid vs. intelligent vehicles. *Trans. Research Part C*, 15, 1–16.

Pisu, P. and Rizzoni, G. (2007). A comparative study of supervisory control strategies for hybrid electric vehicles. *IEEE Transactions on Control Systems Technology*, 15(3), 506–518.

Sciarretta, A., Back, M., and Guzzella, L. (2004). Optimal control of parallel hybrid electric vehicles. *IEEE Transactions on Control Systems Technology*, 12(3), 352–363.

Stoicescu, A.P. (1995). On fuel-optimal velocity control of a motor vehicle. *International Journal of Vehicle Design*, 16(2/3), 229–256.

Tomiyama, K. (1985). Two-stage optimal control problems and optimality conditions. *Journal of Economic Dynamics and Control*, 9, 317–337.

van Keulen, T., de Jager, B., Foster, D., and Steinbuch, M. (2010). Velocity trajectory optimization in hybrid electric trucks. In *2010 American Control Conference*.

Wei, X., Guzzella, L., Utkin, V.I., and Rizzoni, G. (2007). Model-based fuel optimal control of hybrid electric vehicle using variable structure control systems. *Jrnl. of Dynamic sys., Measurement, and Control*, 129, 13–19.

Wipke, K.B., Cuddy, M.R., and Burch, S.D. (1999). Advisor 2.1: a user-friendly advanced powertrain simulation using a combined backward/ forward approach. *IEEE Trans. on Vehicular Technology*, 48(6), 1751–1761.

Zhuang, P., Qi, Q., Shang, Y., and Shi, H. (2008). Model-based traffic prediction using sensor networks. In *5th IEEE Consumer Communications and Networking Conference*.